

SIGNAL COHERENCE MODEL FOR WIDELY SPACED  
SENSORS IN SHALLOW WATER WITH ROUGH BOUNDARIES

J. M. Ozard\* and B. C. Zelt\*\*

\*Defence Research Establishment Pacific,  
FMO, Victoria, B.C., CANADA V0S 1B0

\*\*Physics Department, University of B.C. CANADA V6T 1W5

ABSTRACT

A model based on normal modes has been developed to predict signal coherence for a sound source in a shallow water waveguide with rough boundaries. Deterministic amplitudes and phases are calculated from a normal mode model and random phase or amplitude fluctuations are added. The model assumes that the mode phase fluctuates as a result of the water boundary roughness and that the fluctuations have a degree of independence that may be chosen arbitrarily. This independence is intended to account for the effect of large sensor separations. Receivers may be in any configuration but the source is restricted to the limiting cases of motions that either maintain the source-receiver range constant or change it by many wavelengths during the coherence estimation period. When the source-receiver range is changing rapidly and the receivers are closely spaced, it is found that the signal coherence depends only on receiver separation, mode shape and mode excitation. For closely spaced sensors broadside configurations give consistently high signal coherence. However, for widely spaced sensors and/or sources that maintain a constant source-receiver range the roughness parameters can have a profound effect on coherence. It is also found that certain configurations may be used to isolate the effect of the various model parameters, and hence may be used to measure these parameters experimentally.

SOMMAIRE

Un modèle, basé sur les modes normaux, a été développé pour prédire la cohérence d'une source sonore située en eau peu profonde limitée par des surfaces irrégulières. L'amplitude et la phase d'un signal certain sont calculées à partir du modèle à modes normaux; des variations aléatoires d'amplitude et de phase sont ensuite ajoutées. Le modèle assume que les fluctuations de phase du mode sont introduites par l'irrégularité des surfaces du guide d'onde, et qu'elles possèdent un degré d'indépendance arbitrairement choisi. Cette indépendance est prévue afin d'inclure le cas des récepteurs grandement espacés. La disposition des récepteurs ne comporte aucune restriction. La source, cependant, est contrainte aux déplacements pour lesquels la distance la séparant du récepteur est constante, ou pour lesquels la distance varie de plusieurs longueurs d'onde à l'intérieur de la période requise pour l'estimation de la cohérence. Lorsque la distance entre la source et le récepteur varie rapidement et que les récepteurs sont faiblement espacés, il est observé que la cohérence est fonction de la séparation entre les récepteurs, de la forme du mode et de son excitation. Pour des récepteurs peu distancés, une configuration dont la direction de la source est perpendiculaire aux récepteurs procure une très grande cohérence. Dans le cas où l'espacement est grand et/ou que la distance "source-

récepteur" est maintenue constante, l'irrégularité des limites du guide d'onde a un effet considerable sur la cohérence. Il est également observé que certaines configurations peuvent être utilisées afin d'isoler l'effet de chaque paramètre et ainsi en déterminer expérimentalement leurs valeurs.

## INTRODUCTION

This paper describes a numerical model for predicting signal properties for a sound source in a shallow layer of water that is bounded by rough surfaces. We also present samples of calculated signal coherence. Coherence is a measure of the similarity of signals at two separate sensors. When signal coherence is high at two separate locations, signals at those locations can usually be processed simply to improve signal-to-noise ratio. Our model can be used in developing more sophisticated array processing schemes that produce greater improvements in signal-to-noise ratio. Such arrays have possible applications in numerous areas, including underwater tracking of, and communication with, submerged survey vessels. Biological sound sources might also be tracked with such arrays. Any situation where the sound wavelength is comparable to the depth of the sound transmitting medium will be subject to similar effects.

During the past twenty years numerous measurements of signal coherence have been reported for underwater sound. Coherences or rates of phase change have been investigated for frequencies from 15 Hz to 13 kHz, at ranges from tens to thousands of miles and at a variety of water depths.<sup>1,2,3,4</sup> Models based on ray theory or normal mode theory, which have been used to predict or explain measured signal coherence, are equally numerous.<sup>5,6,7</sup> These models are restricted to specific types of roughness or propagation conditions. Despite the wide range of measurements and the various theoretical models, signal coherence at low frequencies in shallow water has not yet received sufficient consideration.

Our interest in shallow water signal properties is derived from a desire to design, and to simulate the performance of, acoustic arrays operating at low frequencies in shallow water. These arrays are intended to detect and localize weak signals in background noise. It is therefore necessary to know the effect of the transmitting medium on such signals. At one shallow water Arctic location, it has been shown that the sound propagation fits a normal mode model at low frequencies and that only two modes propagate effectively.<sup>8</sup> However insufficient information is available to describe the fluctuations induced by the ice cover.

In a regime with only a few modes present, either a deterministic or a statistical approach, working directly from the bottom profiles and ice surface profiles, could be attempted. Instead, to make the problem more tractable, we assume that the roughness coupled with source motion has produced fluctuations of mode amplitude or of mode phase but not both. The statistical distribution of mode amplitude or mode phase is our starting point. We assume a family of such distributions, rather than a particular distribution, in an attempt to give the results more general significance. It should be emphasized that the model does not relate coherence directly to the roughness of the waveguide boundaries. Our model is a parametric model insofar as the fluctuations are concerned and thus enables testing of array processing schemes for a variety of possible fluctuation distributions when the roughness of the boundaries is unknown.

The model enables a calculation of coherence for arbitrary excitation of the normal modes, since source depth affects mode excitation, this allows any source depth to be treated. By introducing a degree of independence to the fluctuations, as measured at the receivers, coherences for sensor pairs in any orientation, and of arbitrarily large separation, can be modelled. Source motions modelled are such that during the coherence estimation period either the range to the receivers changes by very much less than one wavelength or by very many wavelengths. Many practical situations can be treated despite these restrictions on source motion. Nevertheless, by using an entirely numerical model, it would be possible to remove the restrictions on source motion but at the expense of greatly increased computation time. A more numerical approach is being used to investigate high resolution beamforming and has enabled cases with more modes to be modelled.<sup>9</sup>

In addition to aiding in array design and simulation of array performance, the model indicates what might be encountered in an experiment to measure signal coherence and so indicates how to go about the measurements. Furthermore, there is a rationale for explaining and categorizing the experimentally determined coherencies.

### I. THEORY

The situation modelled, and the physical parameter values used to calculate the numerical values presented here, are shown in Figure 1. Sound from the monochromatic point source is received by a pair of hydrophones whose positions within the water column are completely arbitrary. The propagation of the sound is modelled as a

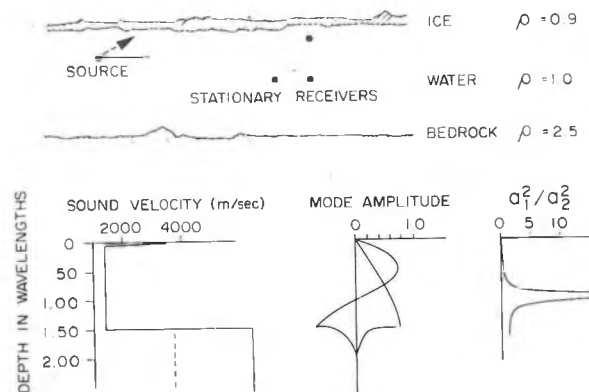


Figure 1. The geometry and geophysical parameters of the coherence model are shown. In the model the source is permitted to move either in the plane of the figure, perpendicular to it or along any intermediate path as long as the path is horizontal.  $a_1^2/a_2^2$  is the ratio of the square of the mode amplitudes at 14.5 Hz.

deterministic part consisting of trapped normal modes with an added statistical components consisting of phase (or amplitude) fluctuations. These fluctuations are attributed to the rough ice surface on the water, the rough bottom, and local variations of sound speed in the water.

To describe sound propagation at a range of more than one wavelength in water, of about one wavelength depth, many rays would have to be included in a ray model. In contrast only a few modes are required to describe the propagation with consequent economies of computation. Thus modes represent the effect of summing over numerous rays. Modes can also be thought of as the interference between upgoing and downgoing acoustic waves as they zigzag between surface and bottom and propagate horizontally. This super-position of two waves traveling in different directions is analogous to a standing wave on a plucked string. Therefore, it is not surprising that the amplitude distribution for the normal modes shown in Figure 1 resembles that of a plucked string. However, the normal mode amplitudes for sound in water do not become zero at the bottom because the impedance contrast at the bottom is not large enough to prevent some motion in the bottom.

The amplitudes for the modes were calculated for a solid ice layer 2 m thick overlying water with a solid bottom. Velocities employed in the calculation were measured with a refraction survey. They represent a very hard bottom thought to consist of a layer of recrystallized dolomite. Only a thin layer (about 1 metre) of unconsolidated material overlies the bottom because of the high currents prevailing in the water. At low frequencies such a layer, be it ice on the surface or till on the bottom, has only a small effect on the deterministic portion of the modes if the layer is thin and smooth. If the layer is randomly rough it will produce mode phase fluctuations similar to those produced by rough ice. The precise nature of the effect of a periodic bottom roughness is a subject that is still under investigation but probably quite different from that of a randomly rough surface.

The wave equation was solved by finding the eigenvalues for a bounded uniform-depth waveguide. For the low frequency results presented, only two trapped slowly moving modes are present. In the modal analysis, energy travelling at higher speeds is carried in the bottom and for such means of transmission, little energy is found in the water column. It has been confirmed by experiment that the amount of energy propagated at these higher speeds is relatively insignificant compared to that propagated in the slowly moving modes.<sup>8</sup> For simplicity, the fast moving modes are ignored and only the slowly moving modes are included in the model.

#### A. Coherence Assuming Mode Phase Fluctuations

The fluctuation distribution to be described next allows control of the fluctuation distribution width and the dependence of fluctuations at sensors with spatial separation. To do this the mode phase fluctuations were formed as a linear combination of fluctuations from distributions of the form,<sup>10</sup>

$$P(x) = \exp(K\cos x) / (2\pi I_0(K)) \quad -\pi \leq x \leq \pi \quad (1)$$

where  $I_0(K)$  is the zeroth order modified Bessel Function of the first kind. This distribution ranges from a uniform distribution for  $K=0$ , to an infinitely narrow

distribution, i.e. known phase, when  $K=\infty$ . Figure 2 illustrates the shape of the

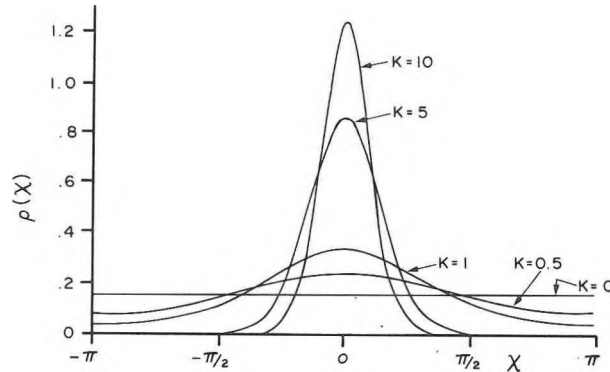


Figure 2. The distribution shown is the one from which the phase or amplitude fluctuations distributions are formed. The parameter  $K$  decreases with increasing roughness.

distribution for several values of  $K$ . It can be seen that for  $K=10$  the effective width of the distribution has narrowed considerably from that for  $K=0$ . If theoretical fluctuation distributions are available for conditions similar to those encountered in a problem of interest, then these theoretical distributions are a guide to likely  $K$  values. When we evaluated  $K$  for one model corresponding to a sea swell on water,<sup>9</sup> and the physical conditions of Figure 1, values of  $K$  between 2 and 75 were obtained for RMS surface roughnesses between 1.0 and 0.1 m. Note that rough surfaces correspond to small values of  $K$ .

To simplify the analysis for the model described here  $K$  was purposely chosen to be identical for the two modes. Although the value of  $K$  for each mode is likely to be somewhat different in practice the conclusions that we draw here are not significantly changed by this simplification. However a more numerical approach can be taken in which  $K$  varies from mode to mode.<sup>9</sup>

$\theta_{ki}$  is used to represent the fluctuating component of the signal phase at the range of hydrophone  $k$  for the component of signal energy travelling as mode  $i$ . This phase fluctuation is defined for frequency  $\omega$ . The fluctuation is written as a linear combination of two independently distributed phases  $u_i$  and  $v_i$ , where  $u_i$  and  $v_i$  are distributed as given by Equation (1). Thus

$$\begin{aligned} \theta_{1i} &= 2(u_i + nv_i)/(1 + n) \\ \theta_{2i} &= 2(v_i + nu_i)/(1 + n) \end{aligned} \quad (2)$$

When  $n = 1$  the fluctuations at separated receivers are identical. While values of  $n$  near zero indicate fluctuations that are independent at the two receivers. Although it is generally recognized that signal coherence decreases with increasing sensor spacing there is insufficient data on the subject to determine suitable values for  $n$ .<sup>11</sup> Thus it is with a view to enabling an investigation of the effect of independence of the fluctuations at separated receivers that the parameter  $n$  is introduced. Whereas the parameter  $K$  depends on the roughness of the sea surface, and decreases with increasing roughness,  $n$  depends on the spatial correlation of the rough surface. At receiver 1 the output will be:

$$Z_1(\omega) = \exp(j\omega t) \sum_{i=1}^N \underline{A}_i \underline{B}_i \underline{X}_i(\omega) \exp(j\theta_{1i}) \quad (3)$$

Where,

- $i$  = mode number with 1 used for the lowest order mode
- $\underline{A}_i$  =  $a_i \exp(j\phi_i)$ , where  $a_i$  is the mode amplitude at the source depth and  $\phi_i$  is the deterministic part of the mode phase at receiver 1 range,  $\phi_i$  equals the product of the range and the horizontal mode wavenumber.
- $\underline{B}_i$  =  $b_i$  the  $i$ th mode amplitude at receiver 1 depth
- $\underline{X}_i(\omega)$  = source amplitude at frequency  $\omega$ .

$\underline{A}_i$ ,  $\underline{B}_i$ ,  $\underline{C}_i$  and  $\underline{X}_i$  are underlined to distinguish these quantities from those used in Equation (5).

The output at receiver 2 depends on  $\theta_i$  where,

$\underline{C}_i$  =  $c_i \exp(j\theta_i)$ , where  $c_i$  is the mode amplitude at receiver 2 depth and  $\theta_i$  is the mode phase shift between the receivers.

The signal coherence squared  $\gamma^2(\omega)$  was calculated by evaluating the integrals required to find the expected values signified by  $E$  where:

$$\gamma^2(\omega) = |E(Z_1(\omega) Z_2^*(\omega))|^2 / (E|Z_1(\omega)|^2 E|Z_2(\omega)|^2), \quad (4)$$

as described in Appendix A. Thus for two modes if we assume that the source-receiver range changes by very much less than one wavelength, i.e. the range remains essentially constant, then,

$$\gamma^2(\omega) = \frac{|MG^2 a_1^2 b_1 c_1 \exp(-j\theta_1) + A^2 B^2 M^2 (a_1 b_1 a_2 c_2 \exp(j(\phi_1 - \phi_2 - \theta_2)) + a_2 b_2 a_1 c_1 \exp(j(\phi_2 - \phi_1 - \theta_1))) + MG^2 (a_2^2 b_2 c_2 \exp(-j\theta_2))|^2}{[a_1^2 b_1^2 + 2A^2 B^2 M^2 a_1 b_1 a_2 b_2 \cos(\phi_1 - \phi_2) + a_2^2 b_2^2] \cdot [a_1^2 c_1^2 + 2A^2 B^2 M^2 a_1 c_1 a_2 c_2 \cos(\phi_1 - \phi_2 + \theta_1 - \theta_2) + a_2^2 c_2^2]} \quad (5)$$

where  $A$ ,  $B$  and  $G$  are functions of  $n$  and  $K$  as defined in Appendix A and  $M=1/(4\pi^2 I_0^2(K))$ .

In the event that source motion is such as to change the range to the receivers by very many wavelengths during the coherence estimation period, then a further integration is required over the variable  $\phi_1 - \phi_2$  in the evaluation of the expected value of the signal coherence. For typical shallow water situations the source would have to traverse of the order of a kilometre during the estimation. When the integrations are carried out over a very large or integral number of periods, terms in Equation (5) that contain  $\phi_1 - \phi_2$  will have dropped out, other terms in Equation (5) remain unchanged. For  $n = 1$  in Equation (2), fluctuations are identical at the two receivers and  $MG^2 = 1$ , so that signal coherence does not depend on the value of  $K$ . This situation would arise with source motion towards closely spaced sensors.

#### B. Coherence Assuming Mode Amplitude Fluctuations

A version of the model for calculating signal coherence for a moving source was developed that assumed mode amplitude fluctuations caused by boundary roughness. To allow independence of these fluctuations at the two receivers the mode amplitude  $a_{ki}$  is written as a linear combination of two independently distributed amplitudes  $e$  and  $f$ , whose squares are distributed like  $x^2$  in,

$$P(x^2) = \exp(K\cos(\pi(x^2 - \alpha)/\alpha)) / 2\alpha I_0(K) \quad 0 \leq x^2 \leq 2\alpha \quad (6)$$

For receiver 1,

$$a_{1i} = (e + nf)$$

and for receiver 2,

$$a_{2i} = (f + ne)$$

where  $i$  indicates the mode number. Choosing the total energy radiated by the source into the two modes to be unity,

$$a_{12}^2 = 1 - a_{11}^2 \quad (8)$$

and,

$$a_{22}^2 = 1 - a_{21}^2.$$

Now the signal at receiver 1 is,

$$Z_1(\omega) = \exp(j\omega t) \sum_{i=1}^N \frac{A_{1i} B_i X_i(\omega)}{A_{1i} B_i X_i(\omega)} \quad (9)$$

where  $A_{1i} = a_{1i} \exp(j\phi_i)$  and otherwise the definitions for Equation (3) apply. Signal coherence squared, Equation (4), was evaluated by carrying out the necessary integrations as described in Appendix B.

Thus

$$\gamma^2(\omega) = \frac{| S_1 b_1 c_1 \exp(-j\theta_1) + S_2 b_1 c_2 \exp j(\phi_1 - \phi_2 - \theta_2) + S_2 b_2 c_1 \exp j(\phi_2 - \phi_1 - \theta_1) + S_3 b_2 c_2 \exp(-j\theta_2) |^2}{[S_4 b^2 + (1 - S_4) b_2^2 + 2S_5 b_1 b_2 \cos(\phi_1 - \phi_2)] \cdot [S_4 c_1^2 + (1 - S_4) c_2^2 + 2S_5 c_1 c_2 \cos(\phi_1 - \phi_2 + \theta_1 - \theta_2)]} \quad (10)$$

where  $S_i = S_i(n, K)$  as defined in Appendix B. For source motion such that source-receiver range is changing by very many wavelengths during the coherence estimation period, terms containing  $(\phi_1 - \phi_2)$  in Equation (10) will have dropped out.

### C. Calculation of coherences

The geophysical parameter values used to calculate the signal coherences in this paper are given in Figure 1. They represent a water layer 1.5 wavelengths deep capped by rough ice. The bottom is modelled as one layer characterized by high compressional wave velocities. The velocity used in this model is based on an unreversed refraction survey and a reflection survey carried out in a Canadian Arctic channel.

Three values of the ratio of the energy in the first mode to the energy in the second mode were used in the coherence calculations. The values were 0.1, 1.0 and 9.0, which occur for source depths near the surface, near the bottom and near the zero of the second mode respectively, as can be seen from Figure 1. The depths associated with the ratios assume no mode conversion or attenuation.

Although the evaluation of Equations (5) and (10) is well within the capabilities of modern computers some care must be taken in evaluating products such as  $A^2 B^2 M^3 G^2$  which are implicit in Equations (5) and (10) and defined in the appendices. For large  $K$  the order of calculation must be such that underflow or overflow are avoided.  $I_n(K)$  was calculated by using coefficients taken from the Handbook of Mathematical Functions.<sup>12</sup> The integrals A, B, D and G were evaluated using Simpson's rule while the double integrals F, G, and H were evaluated by using Patterson's method. The mark 8 version of the Numerical Algorithm Group's DOLDAF was used for the double integrals.<sup>13,14</sup>

## II. DISCUSSION OF RESULTS

In Figures 3 to 6, coherences are presented for modes with fluctuating phase. Similar results are obtained for closely spaced sensors if the amplitude of the modes is assumed to fluctuate. In the case of  $n = 1$ , closely spaced sensors, the results for the amplitude case are either identical to or can be scaled from the phase case depending on the source motion.<sup>15</sup> When amplitude fluctuations are assumed and the source-receiver range is constant then scaling is required. Scaling is such that coherences assuming amplitude fluctuations are higher than coherences assuming phase fluctuations. The scaling also depends on the relative energy in the modes. However,

scaling of the distribution parameters does not carry over to the case of widely spaced sensors. Suffice it to say that coherences for amplitude fluctuations are similar to those obtained assuming phase fluctuations.

#### A. Source Moving Towards Closely Spaced Sensors

If a sound source is moving towards closely spaced sensors with only horizontal separation in the direction of sound propagation, modelled coherence is a periodic function of sensor separation. Coherence decreases cosinusoidally from one, at zero horizontal separation, reaching a minimum at a separation of 4.2 wavelengths. This minimum coherence is that displayed on the diagonal in Figure 3. If separations of

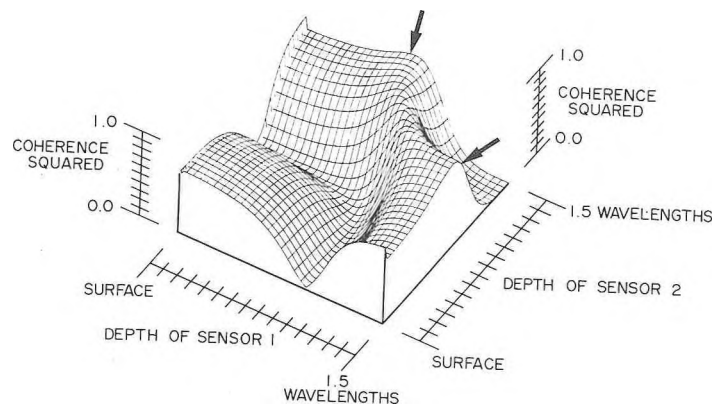


Figure 3. Coherence squared for a source moving towards closely spaced receivers with either mode amplitude or mode phase fluctuating. The sound source is near the bottom in water 1.5 wavelengths deep and the receivers are 4.2 wavelengths apart in the direction of sound propagation.

4.2 wavelengths are well within the close spaced regime ( $n=1$ ), coherence will recover at wider separations because of the cosinusoidal dependence of the coherence. The separation,  $4.2 \lambda$ , at which the minimum occurs is determined by the difference between the mode propagation constants and will vary with frequency.

The coherences in Figure 3 are for closely spaced sensors,  $n=1$ , and represent results for a near-bottom source for sensors whose horizontal component of separation in the direction of sound propagation is 4.2 wavelengths. In the limiting case where the source-receiver range is changing rapidly, as modelled in Figure 3, the results shown apply without regard to whether the fluctuations are of phase or amplitude and there is no dependence on the parameter  $K$  that is used to account for roughness.<sup>13</sup> To completely determine signal coherence for this scenario, it is necessary only to specify source depth, receiver depths, mode shapes, and receiver separation in the direction of sound propagation. Coherences for this scenario are thus determined by modal properties for a smooth waveguide and by the source-receiver geometry.

On the diagonal in Figure 3, for which the depths of sensors one and two are equal, the coherence for a horizontal array of two hydrophones 4.2 wavelengths apart is displayed. These are the worst case coherences for a horizontal array, with sensor separation in the direction of sound propagation, provided that we can assume that the sensors lie in the close-spaced regime.

A special region of perfect coherence, where one receiver is displaced above the depth of the zero of the second mode (one wavelength depth) and the other an almost equal amount below the zero, is indicated by arrows in Figure 3. This includes the special case where both receivers are at the depth of the zero of the second mode, for which coherence is also perfect. The results in the figure indicate that a variation in the depth of one receiver of a very small fraction of a wavelength from the depth of the zero of the second mode will lead to a substantial loss of coherence.

As mentioned earlier coherences for three apparent source depths were calculated. These cases are similar in shape with different emphasis. If the source is near the zero of the second mode the rate of reduction of coherence as the sensors move away from the zero of the second mode will be reduced from that for the near-bottom source depicted in Figure 3. In contrast, for a source in the upper part of the water column the rate of reduction of coherence as the sensors move away from the zero of the second mode will be increased.

#### B. Source-Receiver Range Constant with Closely Spaced Sensors

To calculate coherence for source motion where the range to the receivers is constant, it is necessary to specify the type of fluctuation, the fluctuation distribution width and the source-receiver range. This is in addition to those parameters that determine modal properties and specify receiver geometry and which were the only parameters required when the source was moving rapidly towards closely spaced receivers. Thus coherences for this scenario reflect the effect of surface roughness on signal coherence.

Figure 4 illustrates how coherence depends on the parameter  $K$  that is used to account for roughness and the source-receiver separation in the direction of sound propagation. The source and receivers are near the bottom and the source-receiver range is such that the two modes are 180 degrees out of phase at the first receiver. Coherence is generally poor and decreases with increasing  $K$ , i.e. decreasing roughness. Very different results are obtained if the phase relationship of the modes at the first receiver is changed. Thus the effect of roughness on coherence can be modified dramatically by the range to the receivers. Nevertheless, measurements with closely spaced sensors with the source-receiver range constant could be used to indicate an appropriate value of  $K$  in an experiment to measure signal coherence.

One can see in Figure 4 that when the source is broadside to the receivers (zero receiver separation in the direction of sound propagation) coherence is good regardless of the value of the roughness parameter  $K$ . However, deviations of the receivers by 0.2 wavelengths from a broadside configuration will lead to a considerable loss of coherence at large values of the roughness parameter i.e. nearly smooth waveguide.

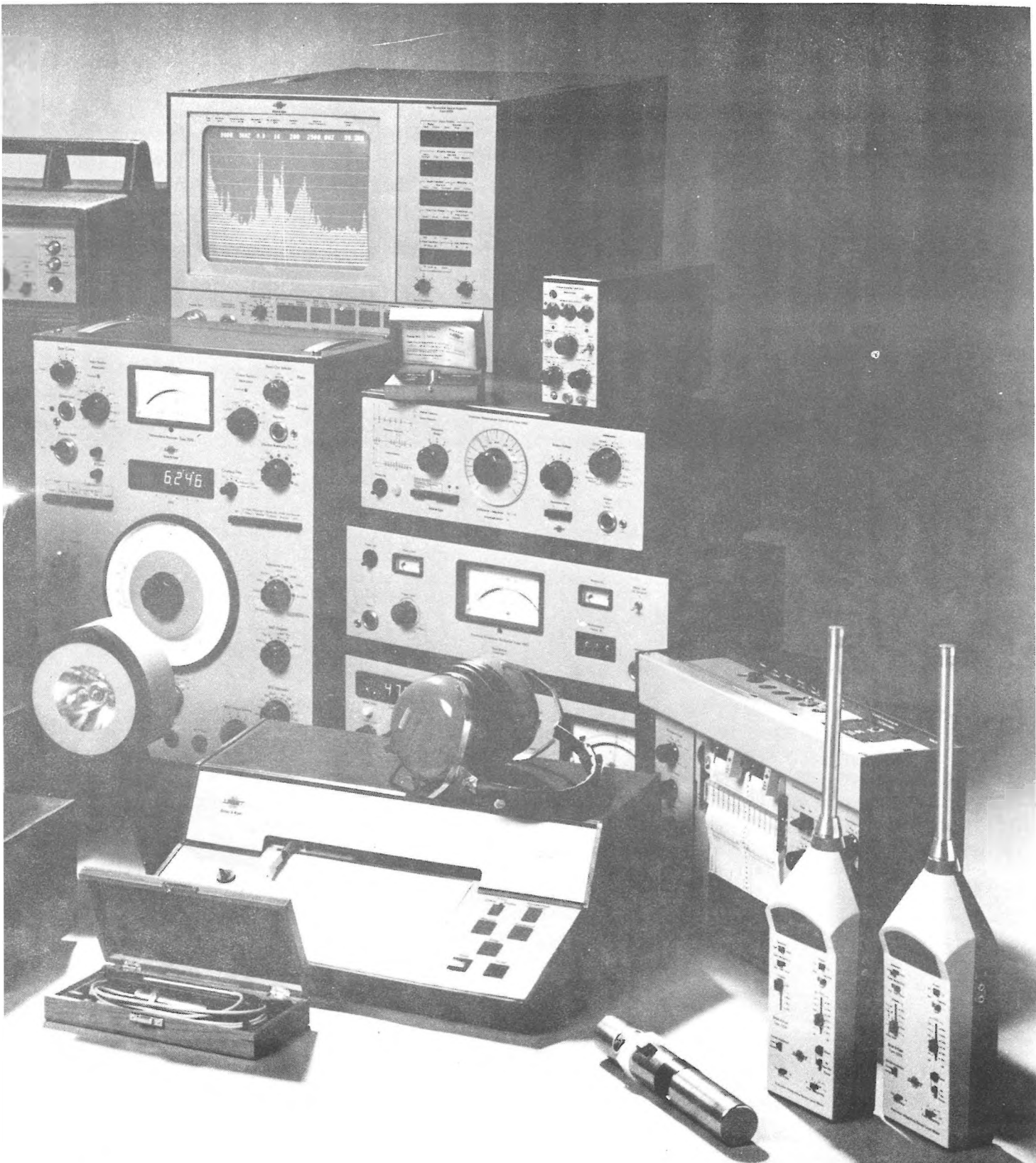
# Keep it all in the family



Everything works together better when you keep it all in the family, especially when it's the Brüel & Kjær family. That's because in our large family of sound and vibration test instruments everything is designed to work together as a total system, from the exciter right through to the display medium or data printer.

So, when you need any instrumentation product from a single transducer to a complete system, check the Brüel & Kjær catalog first, and keep your system all in the family.

For a look at how our family has grown, give us a call.



# BRÜEL & KJÆR CANADA LTD.

## MONTREAL:

Main Office  
90 Leacock Road,  
Pointe Claire, Quebec H9R 1H1  
Tel: (514) 695-8225  
Telex: 05821691 b + k pclr

## OTTAWA:

Merivale Bldg.,  
7 Slack Road, Unit 4,  
Ottawa, Ontario K2G 0B7  
Tel: (613) 225-7648

## LONDON:

23 Chalet Crescent,  
London, Ont.,  
N6K 3 C 5  
Tel: (519) 657-9689

## TORONTO:

Suite 71 d,  
71 Bramalea Road,  
Bramalea, Ontario L6T 2W9  
Tel: (416) 791-1642  
Telex: 06-97501

## VANCOUVER:

5520 Minoru Boulevard, room 202,  
Richmond, BC V6X 2 A9  
Tel: (604) 278-4257  
Telex: 04-357517

### C. Source Moving Towards Widely Spaced Sensors

Figure 5 shows calculated coherences for a source moving towards a broadside array with  $K=0$ , corresponding to a very rough surface. It can be seen that coherence is high when  $n=1$ ; this corresponds to the subset of closely spaced receivers. High coherence was also obtained for the closely spaced regime with a broadside array when the source-receiver range was constant, Figure 4. Both of these results hold true regardless of source depth.

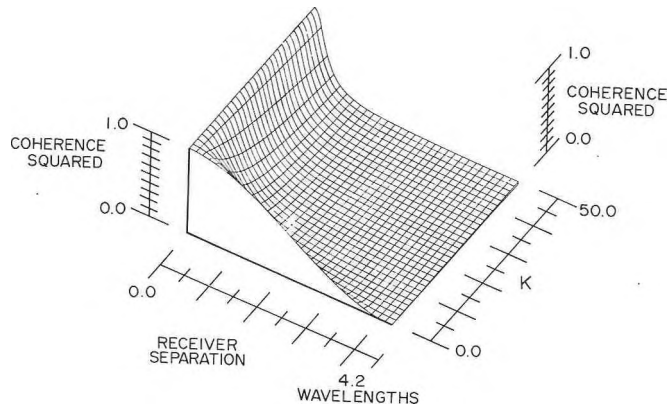


Figure 4. Coherence squared for phase fluctuations and a moving source that maintains constant source-receiver range as it moves horizontally near the bottom. The modes are  $180^\circ$  out of phase at the first receiver,  $a_1^2/a_2^2=1$  and the closely spaced receivers are on the bottom in water 1.5 wavelengths deep. Larger values of  $K$  correspond to smaller values of roughness.

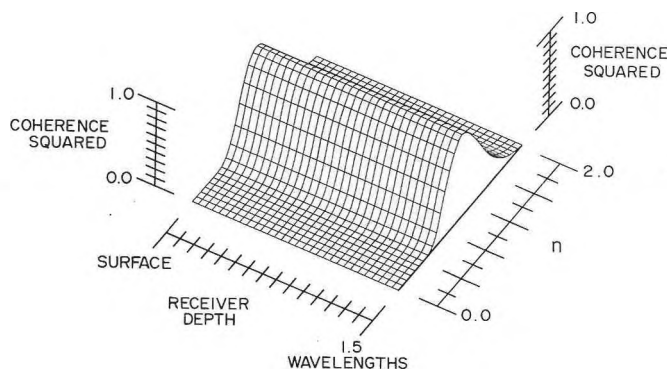


Figure 5. Signal coherence squared for a source moving towards the receivers assuming mode phase fluctuates. The source is broadside to the receivers and near the bottom (1.5 wavelength depth) in a rough waveguide ( $K=0$ ).  $n=1$  corresponds to small receiver spacings and  $|n-1|$  increases with increasing receiver spacing.

The model accounts for more widely spaced sensors by introducing some independence to the fluctuations. As  $n$  increases or decreases from 1 the fluctuations become more independent at adjacent receivers. Figure 5 shows the rate at which coherence drops off with increasing independence of the fluctuations. Coherence plots for larger  $K$  values are similar to coherences shown in Figure 5 but have values that decrease less rapidly as  $n$  changes from unity.

A value for  $n$  is required to pursue the modelling of signal coherence for the scenario of a source approaching widely spaced sensors. This could be measured with a source approaching a broadside array containing receivers with a variety of separations. From such measurements the relationship between  $n$  and hydrophone separation could be obtained. By analogy with ray acoustics the demarcation between the widely spaced regime and the closely spaced regime would occur for hydrophone separations of the order of the dimensions of the first Fresnel zone at a sound reflection point. Still larger hydrophone separations could lie within the closely spaced regime if the rough surface were strongly correlated over regions larger than the Fresnel zones. These zones have dimensions of many wavelengths and depend on the geometry of the propagation path. However, it is unlikely that the ice surface roughness would be strongly correlated over regions exceeding the size of the Fresnel zones.

#### D. Source-Receiver Range Constant and Widely Spaced Sensors

When the receivers are widely spaced a constant range can only be approximated for a moving source by using a circular arc at very long ranges. A sample of calculated coherence for this scenario is presented in Figure 6. The sound source is near

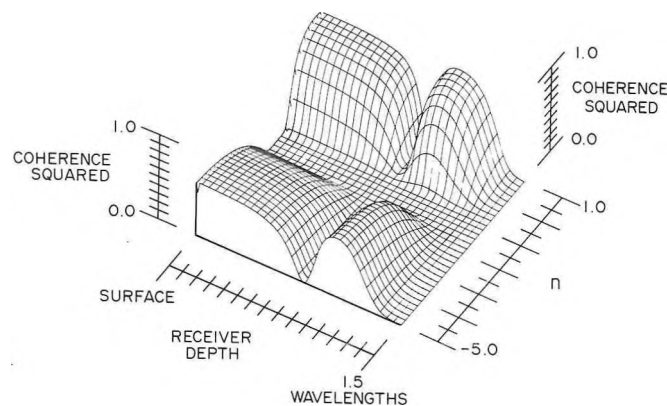


Figure 6. Signal coherence for a sound source moving such that the source-receiver range is constant. The source is near the bottom and the modes are in phase at the first receiver. A receiver separation of 4.2 wavelengths in the direction of sound propagation is assumed and the mode phase is fluctuating. This case corresponds to small roughness ( $K=50$ ).

the bottom, the range is one for which the modes are in phase at the first receiver, and the receivers have a separation of 4.2 wavelengths in the direction of sound propagation. The results show clearly that coherence is dependent strongly on the depth and the independence of the fluctuations at the two receivers. When  $n=0$  fluctuations are completely independent, but, because the roughness is small, ( $k=50$  in Figure 6), the signals received are still coherent. Consequently, a measure of  $K$  might go a long way towards simplifying the range of possible signal coherences.

It is difficult to summarize the results for this particular regime since every parameter in the model has a bearing on the signal coherence. However, provided that the roughness is small enough that  $K$  is large, the independence of the fluctuation will have moderate effect on the coherence. Furthermore, if the source is broadside to the receivers and all other parameters remain the same higher coherences are generally obtained.

### E. Discussion of Results

Coherences calculated with the model, fall into four major categories determined by whether the coherences are for closely or widely spaced sensors and whether source-receiver range is constant or varying. Table I indicates those parameters that

TABLE I. Properties of Coherence Squared.

	SOURCE-RECEIVER RANGE CHANGING RAPIDLY	SOURCE-RECEIVER RANGE CONSTANT
	INDEPENDENT OF FLUCTUATION DISTRIBUTION	AMPLITUDE FLUCTUATION CASE SCALES FROM PHASE CASE
	DEPENDS ON:	DEPENDS ON:
CLOSELY SPACED SENSORS	- MODE SHAPES - SOURCE DEPTH - RECEIVER GEOMETRY	- MODE SHAPES - SOURCE DEPTH - RECEIVER GEOMETRY - DISTRIBUTION WIDTH - FLUCTUATION TYPE - SOURCE-RECEIVER RANGE
	DEPENDS ON:	DEPENDS ON:
WIDELY SPACED SENSORS	- MODE SHAPES - SOURCE DEPTH - RECEIVER GEOMETRY - DISTRIBUTION WIDTH - FLUCTUATION TYPE - DISTRIBUTION DEPENDENCE	- MODE SHAPES - SOURCE DEPTH - RECEIVER GEOMETRY - DISTRIBUTION WIDTH - FLUCTUATION TYPE - SOURCE-RECEIVER RANGE - DISTRIBUTION DEPENDENCE

we must specify to calculate coherence. In the limiting case, closely spaced sensors and source-receiver range changing rapidly, signal coherence is completely predictable without knowing the roughness. Only the modal properties for a smooth waveguide and the receiver geometry are required to determine signal coherence. In contrast, the number of parameters that must be specified and the variety of possible results is greatest for a widely spaced endfire array with a source moving so that the source-receiver range is constant.

The model indicates how one may systematically go about measuring signal coherences at low frequencies. The simplest case of a closely spaced endfire array with the source moving towards the receivers would essentially indicate how the energy is distributed between the modes. Next a constant source-receiver range with a closely spaced endfire array would enable the roughness parameter  $K$  to be established. Lastly an array operating in the wide spaced regime would be used to evaluate the parameter  $n$ .

Without supporting measurements the model has indicated the effect of source motion and receiver geometry on signal coherence. It appears that a source in the broadside position is likely to produce coherent signals at receivers many wavelengths apart. Experimental measurements would indicate at just what receiver separation the value of  $n$  is reduced so that we have reached the wide spaced regime and therefore, if  $K$  is sufficiently small, the spacings at which coherence is poor.

Another approach to narrowing the range of possible predicted coherences is that of modelling the propagation in detail to evaluate  $K$  and  $n$  from the roughness. A theoretical investigation of the effect of roughness on modal properties is being carried out by G.H. Brooke of this establishment that should lead to the equivalent of a relationship between  $K$  and roughness. Evaluation of  $K$  for a given roughness for surfaces that are not near the small roughness limit is no small task and finding  $n$  for a rough surface is even more difficult. However, knowledge of the effect of roughness on signal properties is important for the prediction of array performance especially where the array is to be used to distinguish targets on the basis of depth, range or bearing.

## CONCLUSIONS

A normal mode model for predicting signal coherence for a moving target in shallow water with rough boundaries has been described. The roughness was taken into consideration by introducing fluctuating mode phase or mode amplitude.

Coherences were calculated for two modes in water 1.5 wavelengths deep bounded by a hard single layer bottom. Calculated coherences for source motion towards closely spaced receivers were independent of the roughness or type of fluctuation assumed. Signal coherence was however strongly dependent upon roughness for widely spaced sensors and a source maintaining a constant range to the receivers. It turned out that a broadside source showed high coherence for closely spaced sensors regardless of the source motion.

The model also indicates how signal coherence might be measured in shallow water so that mode properties and the various effects of roughness can be isolated and measured. Such measurements would enable the appropriate values of the model parameters to be identified. A direct approach for predicting the effect of measured roughness on mode properties might also enable appropriate values of the model parameters to be identified.

## ACKNOWLEDGMENTS

The authors wish to thank their DREP colleagues especially Dr. G.H. Brooke for useful discussions.

## REFERENCES

1. G.H. Robertson and R.L. Wagner, "Low-Frequency CW Coherence Measurements for Long Underwater Paths", J. Acoust. Soc. Am., 68, 941-951, (1980).
2. J.C. Steinberg and T.G. Birdsall, "Underwater Sound Propagation in the Straits of Florida", J. Acoust. Soc. Am., 39, 301-315, (1966).
3. R.M. Kennedy, "Phase and Amplitude Fluctuations in Propagating through a Layered Ocean", J. Acoust. Soc. Am., 46, 737-745, (1969).
4. P.N. Mikhalevsky, "Characteristics of CW Signals Propagated Under the Ice in the Arctic", J. Acoust. Soc. Am., 70, 1717-1722, (1981).
5. R. Klemm, "Horizontal Array Gain in Shallow Water", Signal Processing, 2, 347-360, (1980).
6. A.A. Gerlack, "Motion Induced Coherence Degradation in Passive System", IEEE Transactions on Acoustics, Speech, and Signal Processing, 26 (1), 1-13, (1978).
7. R.P. Flanagan, N.L. Weinberg and J.G. Clark, "Coherent Analysis of Ray Propagation with Moving Source and Fixed Receiver", J. Acoust. Soc. Am., 56, 1673-1680, (1974).
8. R.F. MacKinnon, G.H. Brooke, and J.M. Ozard, "Propagation Anomalies in Shallow Arctic Water", J. Acoust. Soc. Am., Suppl. 1, 69, S 19, (1981).
9. J.M. Ozard, I. Barrodale and C. Zala, "High-Resolution Source-Depth Estimation in Ice-Covered Shallow Water", NATO Advanced Study Institute Series, Luneburg Germany 1984 (In press).
10. H.L. Van Trees, "Detection Estimation and Modulation Theory", Part 1, 338, John Wiley and Sons Inc., N.Y., (1968).
11. R.J. Urick, "Principles of Underwater Sound for Engineers", McGraw-Hill, p. 53, 1967.
12. M. Abramowitz and I.A. Stegun, "Handbook of Mathematical Functions", Dover Publications Inc., N.Y., (1965).
13. Numerical Algorithms Group, Fortran Library Manual Mark 8, Subroutine D01DAF.
14. T.N.L. Patterson, Maths. Comp. 27, 847-856 and 877-881, (1968).
15. J.M. Ozard, G.H. Brooke, and M.J. Wilmut, "Signal Coherence Modelling for Shallow Water with Rough Boundaries", Defence Research Establishment Pacific, Technical Memorandum 82-1, March (1982).

APPENDIX A

Signal Coherence for Phase Fluctuations

From Equation (3) and a similar equation for  $Z_2(\omega)$  where  $\underline{C}$  is substituted for  $\underline{B}$  and we ignore source strength for simplicity,

$$\begin{aligned} \overline{Z_1 Z_2^*} &= \underline{A_1 B_1 A_1^* C_1^*} \int_{-\pi}^{\pi} \exp\{2j((1-n)u_1 + (n-1)v_1)/(1+n)\} \cdot \\ &\quad \exp(K\cos u_1 + K\cos v_1) du_1 dv_1 / 4\pi^2 I_0^2(K) \\ &+ \underline{A_1 B_1 A_2^* C_2^*} \int_{-\pi}^{\pi} \int_{-\pi}^{\pi} \int_{-\pi}^{\pi} \exp\{2j(u_1 + nv_1 - v_2 - nu_2)/(1+n)\} \cdot \\ &\quad \exp(K\cos u_1 + K\cos v_1 + K\cos v_2 + K\cos u_2) du_1 du_2 dv_1 dv_2 / 16\pi^4 I_0^4(K) \\ &+ \underline{A_2 B_2 A_1^* C_1^*} \int_{-\pi}^{\pi} \int_{-\pi}^{\pi} \int_{-\pi}^{\pi} \exp\{2j(u_2 + nv_2 - v_1 - nu_1)/(1+n)\} \cdot \\ &\quad \exp(K\cos u_2 + K\cos v_2 + K\cos v_1 + K\cos u_1) du_1 du_2 dv_1 dv_2 / 16\pi^4 I_0^4(K) \\ &+ \underline{A_2 B_2 A_2^* C_2^*} \int_{-\pi}^{\pi} \int_{-\pi}^{\pi} \exp\{2j((1-n)u_2 + (n-1)v_2)/(1+n)\} \cdot \\ &\quad \exp(K\cos u_2 + K\cos v_2) du_2 dv_2 / 4\pi^2 I_0^2(K) \end{aligned}$$

Now let

$$A(n,K) = \int_{-\pi}^{\pi} \exp(j(\pm 2x/(1+n)) + K\cos x) dx$$

$$B(n,K) = \int_{-\pi}^{\pi} \exp(j(\pm 2nx/(1+n)) + K\cos x) dx$$

(A2)

$$G(n,K) = \int_{-\pi}^{\pi} \exp(\pm 2jx(1-n)/(1+n) + K\cos x) dx$$

$$M(K) = 1/(4\pi^2 I_0^2(K))$$

Thus substituting A, B, G, and M in (A1) and similar expressions for  $Z_1 Z_1^*$  and  $Z_2 Z_2^*$  and substituting the result in (4) produces (5).

APPENDIX B

Signal Coherence for Amplitude Fluctuations

From Equation (9) and a similar equation for  $Z_2$  except that  $\underline{C}$  is substituted for  $\underline{B}$ .

$$\begin{aligned} \overline{Z_1 Z_2^*} &= b_1 c_1 \exp(-j\theta_1) n \int_0^{2\alpha} e^2 P(e^2) de^2 + n \int_0^{2\alpha} f^2 P(f^2) df^2 \\ &+ (1+n^2) \int_0^{2\alpha} \int_0^{2\alpha} e f P(e^2) P(f^2) de^2 df^2 \\ &+ b_1 c_2 \exp j(\phi_1 - \phi_2 - \theta_2) \int_0^{2\alpha} \int_0^{2\alpha} (e + nf) \{1 - (e + nf)^2\}^{1/2} P(e^2) P(f^2) de^2 df^2 \\ &+ b_2 c_1 \exp j(\phi_2 - \phi_1 - \theta_1) \int_0^{2\alpha} \int_0^{2\alpha} (f + ne) \{1 - (f + ne)^2\}^{1/2} P(e^2) P(f^2) de^2 df^2 \\ &+ b_2 c_2 \exp(-j\theta_2) \int_0^{2\alpha} \int_0^{2\alpha} \{1 - (e + nf)^2\}^{1/2} \{1 - (f + ne)^2\}^{1/2} P(e^2) P(f^2) de^2 df^2 \end{aligned}$$

let  $x$  or  $y = e^2$  or  $f^2$  as appropriate, and

$$D = \int_0^{2\alpha} x^{1/2} P(x) dx \quad (B2)$$

$$G = \int_0^{2\alpha} \int_0^{2\alpha} (x^{1/2} + ny^{1/2}) \{1 - (y^{1/2} + nx^{1/2})^2\}^{1/2} \exp(-K\cos(\pi x/\alpha) - K\cos(\pi y/\alpha)) dx dy \quad (B3)$$

$$H = \int_0^{2\alpha} \int_0^{2\alpha} \{(1 - (x^{1/2} + ny^{1/2})^2)(1 - (y^{1/2} + nx^{1/2})^2)\}^{1/2} \exp(-K\cos(\pi x/\alpha) - K\cos(\pi y/\alpha)) dx dy \quad (B4)$$

For the evaluation of  $Z_1 Z_1^*$  and  $Z_2 Z_2^*$  we need to define

$$F = \int_0^{2\alpha} \int_0^{2\alpha} (x^{1/2} + ny^{1/2}) \{1 - (x^{1/2} + ny^{1/2})^2\}^{1/2} dx dy \quad (B5)$$

Now to further simplify the expression for signal coherence, Equation (10), let,

$$\begin{aligned} S_1 &= 2n\alpha + \frac{(1+n^2)D^2}{4\alpha^2 I_0^2(K)} \\ S_2 &= G/(4\alpha^2 I_0^2(K)) \\ S_3 &= H/(4\alpha^2 I_0^2(K)) \\ S_4 &= (1+n^2)\alpha + 2nD^2/(4\alpha^2 I_0^2(K)) \\ S_5 &= F/(4\alpha^2 I_0^2(K)) \end{aligned} \tag{B6}$$

NOW AVAILABLE



# INDUSTRIAL NOISE CONTROL MANUAL

(CAA reprint of the original NIOSH manual)



This MANUAL contains basic information on understanding, measuring, and controlling noise, and more than 60 actual case histories of industrial noise control projects. It is written for persons who have had little or no experience in noise control. Included are sections on noise control, acoustic materials, and the choice of a consultant.

**SINGLE COPIES ..... \$20.00**  
**Volume Discounts Available**

**Send Requests With Payment To :**

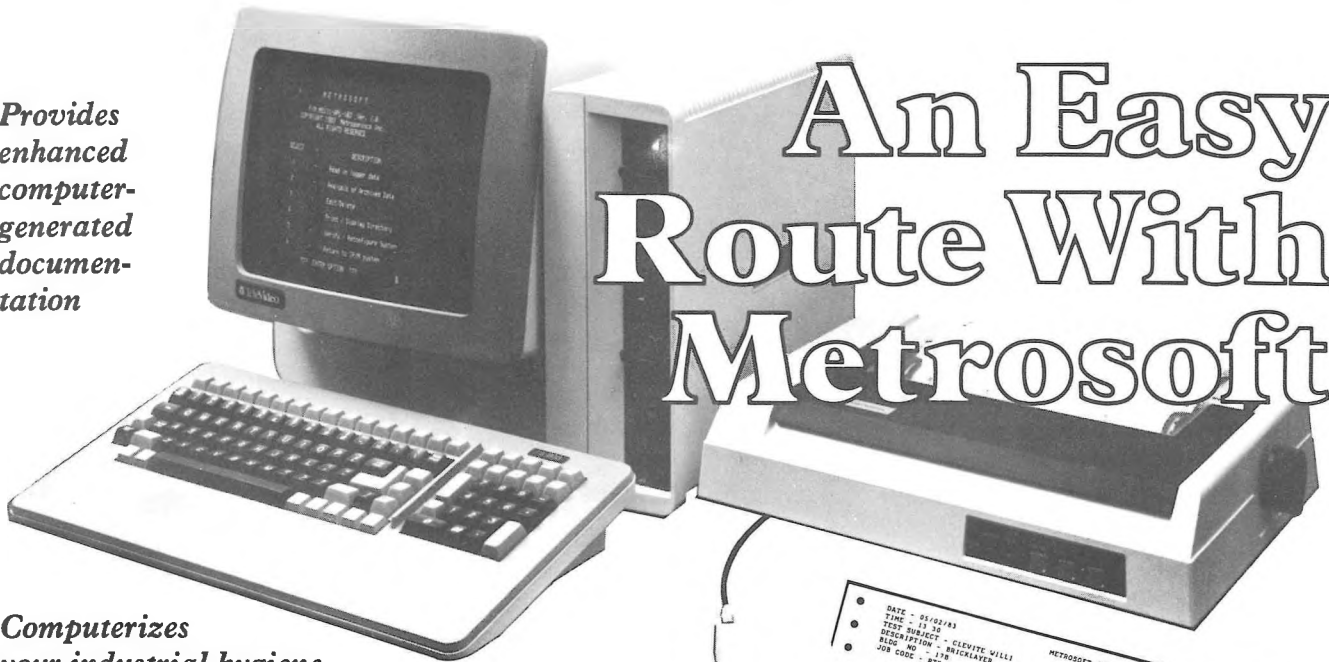
**EXECUTIVE SECRETARY:**

**D.A. Benwell**  
**Health and Welfare Canada, R.P.B.**  
**Environmental Health Centre**  
**Room 233, Tunney's Pasture**  
**Ottawa, Ont.**  
**K1A 0L2**

**(613) 995-9801**

# FROM METROLOGGER® TO PERSONAL COMPUTER...

*Provides enhanced computer-generated documentation*



## An Easy Route With Metrosoft

*Computerizes your industrial hygiene recordkeeping and analysis*

Metrosoft software enables you to transfer industrial hygiene and pollution data directly from Metrologgers to popular personal computers.

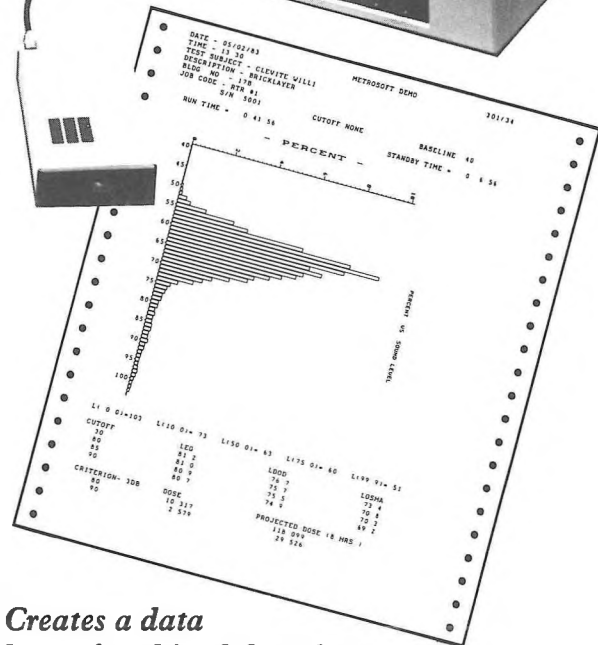
Noise exposure data from db-301 Metrologgers, information on toxic and combustible gases, organic vapors, air contaminants and much more is available from standard environmental monitors, via dl-331 Universal Data Loggers and other compatible instruments.

The hook-up couldn't be more simple. A single cable delivers data directly from logger output to the computer. Metrosoft's floppy disc program takes over from there.

Metrosoft is user-friendly and is menu-driven. It recognizes the type of logger, its program and model number. The operator merely inputs personnel data and identifies the test variable. No prior computer experience is required.

Summary time histories and exposure data are displayed and are available on hard copy; graphs can be plotted in condensed and detailed format. All data is stored on floppy discs, saving filing space.

Sophisticated archiving and search routines give broad flexibility for examining data sub-groups, long after tests are completed. You are allowed four fields



*Creates a data base of archived data for future analysis, correlation and review*

of test identification, enabling you, for example, to call up all measurements of a given variable, in a given location, in a given month. Or, you might simply request all noise dosimetry tests for an individual worker.

Metrosoft is one, neat software package for occupational health surveillance. Call or write today for your copy of our new 4-page brochure.

REPRESENTED IN CANADA EXCLUSIVELY BY



**LEVITT-SAFETY LIMITED**  
33 Laird Drive, Toronto, Ontario M4G 3S9

BRANCHES THROUGHOUT CANADA



**METROSONICS INC.**  
GENERAL PRODUCTS DIVISION  
P.O. BOX 23075 • ROCHESTER, N.Y. 14692 • 716-334-7300

*The New Generation  
Of Noise Analyzers*